NOAA Technical Report ERL 343-SEL 34

U.S. DEPARTMENT OF COMMERCE
NATIONAL OCEANIC AND ATMOSPHERIC ADMINISTRATION
Environmental Research Laboratories

Review of Ionospheric Small Scale Structure With Emphasis on Equatorial Radio Scintillation in the SHF Band

JOSEPH H. POPE
CLIFFORD RUFENACH

BOULDER, COLO.
SEPTEMBER 1975

U.S. DEPARTMENT OF COMMERCE
Rogers C. B. Morton, Secretary

NATIONAL OCEANIC AND ATMOSPHERIC ADMINISTRATION
Robert M. White, Administrator
ENVIRONMENTAL RESEARCH LABORATORIES
Wilmot N. Hess, Director

NOAA TECHNICAL REPORT ERL 343-SEL 34

Review of Ionospheric Small Scale Structure With Emphasis on Equatorial Radio Scintillation in the SHF Band

JOSEPH H. POPE
CLIFFORD RUFENACH

BOULDER, COLO.
September 1975

For sale by the Superintendent of Documents, U. S. Government Printing Office, Washington, D. C. 20402

TABLE OF CONTENTS

REVIEW OF IONOSPHERIC SMALL SCALE STRUCTURE WITH EMPHASIS ON EQUATORIAL RADIO SCINTILLATION IN THE SHF BAND

Joseph H. Pope[1]
Clifford Rufenach[2]

The literature relating to small-scale ionospheric irregularities in electron density observed by in-situ and scintillation methods is examined for possible causes of the high level scintillation activity observed in the equatorial regions in the SHF band. A global scintillation model is extrapolated from the VHF to SHF regions by incorporating the power law irregularity spectrum into existing scintillation theory. The Booker theory that suggests equatorial SHF scintillations may arise from irregularities located well beyond the ionosphere at distances the order of 1 Earth radius is found to be a plausible explanation of the large scintillation levels observed. Such irregularities may be similar to or a subset of the field-aligned ducts observed by topside ionospheric sounders and natural VLF wave propagation. If this theory is confirmed, it will be necessary to model the scintillation in this geographical and frequency region separately from the model based on VHF scintillations.

Other studies reported include a theoretical explanation of an interference pattern observed as a "ringing" on radio beacon records of signals from ATS-6. The theory suggests that the pattern is produced from two-ray interference associated with a large scale steep front change in electron density drifting into the path between the satellite and surface station.

1. INTRODUCTION

Although the effects of irregular structure in the ionosphere on trans-ionospheric radio signals have been under scientific study for a quarter century, only during the past decade, with the development of satellite applications (as in communications), have these effects been of practical importance. The irregular structure, generally considered to be elongated blobs of electron density aligned with the Earth's magnetic field, shifts the phase of radio waves passing through the structure, compared with the phase of radio waves passing through a homogeneous ionosphere. This phase shift results in a corrugated wavefront as the radio wave emerges from the ionosphere, producing a phase interference effect at the surface. The resulting signal has a variation in amplitude and phase similar to the twinkling effect noted in stellar light passing through the atmosphere and has been referred to as scintillation.

---

[1]Now with National Environmental Satellite Service, NOAA.
[2]Now with Atlantic Oceanographic and Meteorological Laboratories, ERL, NOAA.

Until a few years ago, the phenomenon had been studied by means of radio-stellar and satellite signals confined to the VHF band and below. These studies provide a fairly clear understanding of the phenomenon on a global basis and with respect to temporal variations and have provided a basis for modeling the scintillation with respect to a number of input parameters. Results of the early studies indicate that the radio frequency dependence is such that the magnitude of the effect decreases with increase in frequency (F) by $1/F$ to $1/F^2$. Thus as transmitters at S-band and higher frequencies began to be employed for satellite applications the expectation was that scintillation effects would produce few difficulties if any.

This expectation was shown to be incorrect when it was found that the transmissions at 2300 MHz from the lunar base ALSEP often exhibit periods of considerable scintillation. Similar activity was observed on the signals from the COMSAT satellites up to frequencies as high as 6 GHz. The amplitude variation was found to be similar to the scintillations exhibited at lower frequencies but were generally confined to a region within +30° of the geomagnetic equator.

This report provides a review of the scintillation effects with primary emphasis on the GHz scintillations. The study incorporates recent in situ measurements of the ionospheric irregularities into the theory of scintillations. These results then lead to a method of extrapolating the present model of scintillation effects from the VHF band to the GHz frequency band.

Originally the study was conceived as a cooperative program between NASA and NOAA, with each agency supplying approximately half of the total funds committed to the project. The program was undertaken within the Ionospheric Physics Area of the Space Environment Laboratory, a unit within the Environmental Research Laboratories, NOAA. Owing to budgetary problems that arose within the Space Environment Laboratory, the amount of effort that could be devoted to the program and its duration were significantly curtailed.

2. REVIEW OF GIGAHERTZ SCINTILLATION OBSERVATIONS

The first observation of severe scintillation on gigahertz frequencies was in February of 1970 (Christiansen 1971). Observations were made in support of the lunar ALSEP station transmitter on 2278.5 megahertz and received at Ascension Island. The fluctuations were later noticed at several other NASA stations within 30° of the magnetic equator. The phenomenon was found to occur usually between 2000 and 2400 hours local time, and during the periods of the equinoxes. The magnitude of the fluctuations generally ranged between 3 and 4 dB, but occasionally values as high as 13 to 25 dB were reported. The latter figures, however, may be spurious because they may have been caused by signal drop-out resulting from loss of phase-lock. These observations were rather surprising in view of the existing theory regarding scintillation effects; in theory, the magnitude should decrease by $1/F^2$. The

evidence indicated that the scintillations were probably caused by ionospheric irregularities, similar to those that produced scintillations at lower frequencies.

Further observations on scintillation effects were made at 6 GHz by means of the Intelsat III-4 at the Mount Logonaut Satellite Telecommunications Station near Nairobi (Skinner et al., 1971). Scintillation fading was observed several times during the equinoxial period March-May, 1971. Again, most of the fading occurred between 2000 and 2400 hours local time, but occasionally fading was observed as late as 0300 hours.

Observations at a number of stations located near the magnetic equator of scintillation signals from the INTELSAT geostationary satellite at 4 and 6 GHz were reported by Craft and Westerlund (1972). They find that the stations having the largest occurrence rates of scintillation tend to be within ± 20° of the geomagnetic equator, that maxima occur during equinoxes, and that the scintillation activity is greater at night than during the day. Diurnal variations indicate that the scintillations begin 1 and 2 hours after local sunset and continue for several hours. Craft and Westerlund suggest that the onset of the scintillations is related to the sunset in the F region which is 1 or 2 hours after sunset on the ground for the stations involved. They find the magnitudes of the scintillation activities of the two frequencies to be related roughly as the square of the radio wavelength. This frequency dependence tends to rule out the suggestion that these scintillations may be caused by tropospheric effects. Further, the morphology of the scintillations seems to be similar to that observed at lower frequencies in the equatorial regions. They conclude that the irregularities responsible for the scintillations at their frequencies occur in the F region.

Further studies using COMSAT observations at 4 and 6 GHz, reported by Taur (1973, 1974), also show temporal variations indicating that the diurnal maximum tends to occur around 2000 local time. For the 12 stations used in his study, the geomagnetic region in which the GHz scintillations are observed tends to be within ±30° geomagnetic latitude. He finds a tendency to negative correlation between the occurrence of scintillation at these frequencies and magnetic activity similar to the negative correlation that has been obtained in the past for the phenomenon known as spread F that is also believed to result from irregular structure in the ionosphere. He suggests that the frequency-dependence is proportional to the square of the wavelength for frequencies above 4 GHz while those below 4 GHz tend to be proportional to wavelength. Taur suggests that the large scintillations observed at GHz frequencies result from rather thick irregular structure in the ionosphere.

One of the early comparative studies of ionospheric scintillations at widely spaced frequencies using radio-stellar sources was reported by Chivers and Davies (1962). This study was conducted at Jodrel Bank, England, looking northward towards the auroral zone. The authors find scintillations at 1390 MHz that seem to be related to scintillations at 79 MHz.

From the dependence on elevation angle of scintillation amplitude at 1390 MHz, the authors conclude that the scintillations originate from irregular regions in the E layer at about 100 km height. They compare their results with earlier studies made at about 9 GHz in which scintillations caused by tropospheric irregularities were observed. The 1320 MHz scintillations were found to correlate positively with magnetic K-indexes. They find considerable departure from the $1/F^2$ law and suggest that this departure might be caused by absorption at the lower frequency. They fail, however, to consider saturation effects at the lower frequency as a cause of the departure. Although the scintillations at 1320 MHz are somewhat greater than might have been extrapolated from the lower frequencies, the scintillation amplitudes are quite small, generally below a few percent in turns of amplitude index.

The S-band transmitters on ESSA-9 and ITOS-1 made it possible to compare the magnitudes of scintillations at 1695 MHz with the 137 MHz transmissions on the same satellites (Pope and Fritz, 1970, 1971). The scintillation indexes on the S-band frequencies were usually smaller than about 10% and rarely more than 20%. The temporal and other variations on the S-band scintillations were found to compare closely with those at VHF. The ionospheric intersection points of the rays from the satellite to the surface station at Gilmore Creek, Alaska, when S-band scintillations were noted, were found to lie for the most part within the auroral zone. These results indicate that the S-band scintillations are produced by the same or similar ionospheric irregularities that produce the scintillations at VHF and S-band, in agreement with the earlier work of Chivers and Davies, depart considerably from the $1/F^2$ law of scintillation amplitude. The S-band scintillation amplitudes tend to be a factor of about 10 below those observed in the VHF range.

The results of these several studies show that scintillations of significant amplitude at GHz frequencies are observable only in the equatorial regions. Scintillations at these frequencies do occur in the polar regions, but they seldom have amplitudes sufficient to cause practical communication problems. Although small, the scintillations in these higher frequencies are larger than might be expected from the frequency-dependence law that had been derived theoretically and observed experimentally at the lower frequencies. There are, however, a number of reasons why the theoretical frequency-dependence law may not be valid over the wide frequency range between S-band and VHF. One of these is that the scintillations tend to saturate at the lower frequencies during times when scintillations at the higher frequencies are observed. Another reason is that the theoretical developments were based on the incorrect assumption that the irregularity structure could be described by a narrow Gaussian distribution in size. Studies using scintillation (Rufenach 1971, 1972) and in situ measurements (Dyson et al., 1974) have shown that the spectral distribution in size is not Gaussian but is better described by a power law function.

An attempt was made by Pope (1974) to incorporate the in situ results into the Briggs and Parkin (1973) theory. In that study it was shown that the scintillation amplitudes would be maximized for those irregularities that have sizes close to the Fresnel radius. This result accounts for the fact that sizes determined in early studies were later found to approximate the Fresnel radii appropriate to the observational conditions.

3. DETERMINATIONS OF IRREGULARITY PARAMETERS

Since the scintillations received on the surface depend intrinsically on the irregularities in the ionosphere causing the scintillations, it is important to attempt to measure the properties of the irregularities. Until recent years it has been difficult to make such measurements except by means of the scintillations themselves. Parameters to be measured include the magnitude of the electron density fluctuation, the size of the irregularities, their elongation, their height, and other factors pertaining to their orientation and shape. Such determinations have importance not only in terms of scintillation theory but also with respect to the theory of formation of the irregularities.

In principle, it should be quite easy to determine the size of the irregularity by scintillation methods, providing certain assumptions are fulfilled, one of which pertains to weak scatter (the phase shift produced is less than one radian). In the case of observations of a relatively stationary source such as a geostationary satellite or radio star, the size of the irregularities can be related to the period of the fluctuations by means of the geometry pertaining to the height and to their velocity as they drift in the ionosphere. This drift is sometimes referred to as a "wind" but at F layer altitudes the concept of winds becomes tenacious. It is more appropriate to think of the drift in terms of a motion of the plasma across field lines induced by electric fields in the ionosphere. Drift velocities are typically about 100 m per second. In the case of an orbiting satellite, the motion of the irregular scintillation pattern on the surface is induced by the motion of the satellite itself. This velocity is large compared with the velocity associated with the drift of the irregularities and therefore the latter can be neglected. Again, it is necessary either to assume or to measure the height of the irregularities to infer their sizes. In both cases certain assumptions regarding statistical stationarity must be made. Observations from suitably located multiple stations can be used to infer both the height and the sizes. In the case of the stationary source, at least three stations are required since both the magnitude and direction of the velocity need to be determined, while for an orbiting satellite only two stations are required since the velocity of the satellite is known to a high degree of precision.

Radio stellar observations of ionospheric irregularities were conducted by Rufenach (1972) in which the theory developed by Lovelace et al. (1970) was used. Rufenach used the power spectral technique in which the coefficient of the Fourier power spectrum is plotted against irregularity

size. He found that the observations as analyzed departed considerably from what might be expected by the Gaussian distribution assumption used in past work, and he was able to show that a power law in the irregularity size distribution is considerably better than the Gaussian law. He suggested that the irregularities may arise in one way or another from turbulent mechanisms since turbulence theory in general predicts power law spectra distributions in the size parameters.

Using similar methods, Singleton (1974) has confirmed the finding that the spatial spectrum of electron fluctuations is a power law rather than Gaussian. Singleton's results also are consistent with the interpretation that the regularities are elongated along the field line. Additionally, he finds a small elongation perpendicular to the magnetic-meridian plane.

The satellite OGO-6 has provided a means of directly observing the electron density fluctuations in the F region irregularities (Dyson et al., 1974; McClure and Hanson, 1973). Using the retarding potential analyzer, they observed the electron density concentration as a function of time and analyzed these observations in terms of the Fourier spectral components of the fluctuations. These analyses provided measurements over scale size ranges from 70 m to about 7 km. In general, the spectrum was found to be approximated by a power law of the form $A = A_o S^n$ where A is the electron density amplitude, A_o = the amplitude at some arbitrarily specified size, S is the irregularity size, and n is the power spectral index. The average value of n turns out to be 0.95 with a small variation from sample to sample. The index seems to be independent of latitude and other factors although the amplitude at any particular size can vary considerably. At times, however, the spectra observed failed to fit any such simple description and several different types of spectra were observed. But these other types were rare compared with the power law spectrum. In general, the results tend to confirm the determinations made by Rufenach (1972).

4. THE BOOKER EQUATORIAL SCINTILLATION THEORY

Recently, Booker (1975) has theoretically examined the possible alternative explanations for the large scintillations observed in the equatorial region in the SHF band. In this study, Booker has advanced earlier theoretical work (Booker 1958, Bohill 1961) to derive a set of equations from which the magnitudes of the electron density fluctuation scale sizes, to account for the magnitude of the observed scintillations, can be derived as functions of height, size of the irregularities, and frequency of the radio wave. For F region heights (300 km), he finds, for instance, that the magnitude of the SHF scintillations can be explained if we assume an outer scale of the order of 80 m with an rms fluctuation in electron density of the order of $10^{11}/m^3$. From plasma physical arguments he finds that parameters of these magnitudes are not plausible in the ionosphere since the scale size is comparable with the mean free path of ions and the required electron density fluctuations are comparable with the electron density in the F region.

Repeating the calculations for heights pertaining to the magnetosphere, Booker is able to show that the plasma physical objections no longer apply. To make these computations, Booker assumed a model appropriate for magnetospheric heights to 8,000 km. With this model, he finds that amplitude scintillations are primarily produced by irregularities having heights up to about 1 Earth radius (6,000 km). The phase scintillations are produced by the full range of heights up to 8,000 km, the point beyond which it was assumed in the model that no irregularities exist. The resulting scintillations are produced by the phase shift integrated over a large height range so that the thin screen approximations that are usually made for ionospheric scintillations do not apply. For electron densities small compared with the ionization density in the F region (order 10^{-10} electrons/m^3), it turns out that the RMS amplitude perturbations are about 2.5%. The low tranverse diffusion rate with respect to the field lines at such altitudes makes these parameters reasonable. Thus, it would appear that the SHF scintillations can be accounted for by the assumption of field-aligned irregularities located far from the F region.

Although the model assumed is necessarily crude because of a lack of detailed information in the region, the success of the calculations suggests that the model with its associated theory is at least plausible. The present experimental observations of scintillation activity can neither confirm nor deny the hypothesis. The observed correlation between scintillations and other effects considered to be associated with the ionosphere does not necessarily negate the hypothesis. For instance, the correlation between the occurrence of scintillations and the occurrence of the spread-F detected by means of ionosondes could be cited as evidence that the hypothesis fails. But there is no reason to suppose that the existence of spread-F precludes the simultaneous existence of the field-aligned irregularities far out into the magnetosphere; these two phenomena might be, in fact, related.

The existence of field-aligned ducts of electron density perturbations was originally suggested some years ago to account for the discrete closely spaced multiple traces of a type of the VLF phenomenon known as whistlers (Helliwell, Crary, Pope, & Smith, 1956). Numerous studies have been conducted of such field aligned irregularities using VLF observations, and the existence of these field-aligned irregularities is well established. It would appear, however, that this particular type of irregularity is somewhat larger than those hypothesized as producing scintillations by Booker. In addition, these irregularities tend to be observed primarily at mid-latitudes up to about 60° geomagnetic.

Another type of field-aligned irregularity was discovered by the topside sounding satellites Alouette 1, Explorer XX, and Alouette 2 (Muldrew, 1963, 1967). These irregularities may be related to the irregularities that are observed by means of whistlers. They were observed by the satellite HF topside ionosondes that were designed to probe the top of the ionosphere. Occasionally, echoes were observed with time delays such that the signals must have propagated by HF duct wave guides over the field line and returned.

In several respects, the occurrence statistics of these irregularities are similar to those observed using SHF scintillation data. They tend to occur during the nighttime hours, becoming pronounced in occurrence about sunset, and they occur predominantly within ± 35° of the geomagnetic equator. There seems to be an interesting longitudinal effect such that they are observed less often in the longitudes of Hawaii than in those corresponding to South America. Similarly SHF scintillations are less prevalent as observed from Guam than from the South American stations.

Loftus et al., (1966) studied these Hf ducts by means of the Explorer XX satellite. They estimated the size of the ducts to range between 1 and 10 km with the mode of 4 km. The fractional change in electron density was estimated from the radio wave frequency-dependence on the occurrence of ducts. These results indicate that electron density deviations from background usually range between 1.6 and 2.5%. Their determination of diurnal variation of the occurrence of ducting differs somewhat from that of Muldrew (1963) and at the peak, tends to occur between 0500 and 0800. However, this difference may be the result of observing at different radio frequencies.

The similarities in the results of the studies of conjugate ducting and of SHF scintillations suggest that the scintillations may be caused by the same or similar field-aligned irregularities that produce the Hf ducting phenomenon. One possible difference exists in the estimates of size as determined for Hf duction and that suggested by Booker in his irregularity model for SHF scintillations. Booker's estimate of size, however, is simply the size of the Fresnel radius. It does not preclude the possibility of sizes greater than the Fresnel radius, but requires only that irregularities having sizes in the range of Fresnel radius must be present with sufficient electron density variation from ambience. If we assume that the ducts follow the same power law in size as that suggested by Rufenach (1972), then it seems reasonable that the irregularities observed by the scintillation method are, indeed, a subset of those ducts observed by topside sounders.

It will be of considerable practical and scientific importance to establish the Booker theory by experimental observations. Until a definitive experiment can be conducted, the Booker hypothesis must be considered a plausible explanation of the SHF scintillation phenomena observed in the equatorial regions.

5. SUMMARY OF PRESENT SCINTILLATION STUDIES

As part of this contract, a number of studies have been undertaken. These studies have included attempts to understand further the nature of the scattering phenomenon, and attempts to reduce the scientific knowledge of scintillations to a form that will be useful for engineering systems studies of satellite communications.

5.1. Modification To The Fremouw Model

The Fremouw model (Fremouw and Rino, 1973) failed to fit the northern hemisphere data obtained by several studies (Aarons, 1973, Aarons and Allen, 1971, and Joint Satellite Studies Group, 1968). More recently, Sagalyn et al. (1974), using in situ satellite data found that the northern and southern polar irregularity boundary regions are not symmetrical, the southern region being about 4 to 5° closer to the pole than the northern region. The reason for this discrepancy is still speculative, but it suggested a reason that the Fremouw model failed to adequately represent certain features of the data since Fremouw had averaged the northern and southern pole regions together under the reasonable assumption that these two regions should be approximately symmetrical. To remove this discrepancy, the northern and southern regions were modeled separately. Certain coefficients in the model were adjusted to accomplish this, resulting in an excellent agreement with the past data (Pope 1974a, 1974b). In addition to these changes of the coefficients, certain changes in the model were made to account for the experimental finding that the boundary tends to decrease in latitude during times of high magnetic activity (Aarons 1973). Another change was made to account for the fact that the line of symmetry of the boundary region, looking at it from the pole, is not the noon-midnight line, but is shifted by about 15° toward the morning side.

Although the agreement between the modified model and the experimental data is improved by this technique, further work by Whitney, AFCL (Fremouw, 1974), indicates a possibility that other modifications may be desirable. In the initial development of the model, it had been assumed that the scintillation index (SI) used by Whitney and others, in analyzing scintillation data over the years, is approximately that given by Briggs and Parkin (1963) as S_3. By comparing the two from the same set of data, Whitney finds the relationship between these two indexes is not linear as had been assumed in the past. If these preliminary results are confirmed, it may be desirable to continue modifying the model. Fremouw is now attempting such modifications at the Stanford Research Institute.

5.2. Effects of the Power Law Irregularities On The Fremouw Model

Another attempt (Pope 1974c) at improving the model was based on the finding by Rufenach (1972) and others that the power law in the spectral distribution of irregularity sizes is a better description than the previously used gaussian distribution. The impact of this determination is that the frequency dependence as determined by Briggs and Parkin (1963), is not strictly correct, since the scale sizes responsible for the observed scintillations depend upon the radio frequency of observation. Therefore, the experimental determinations of the size distribution (Dyson et al., 1974) were inserted into the Brigg and Parkin theory to attempt model revisions.

Figure 1 shows the frequency dependent portion of the Briggs and Parkin (1963) theory after insertion of the power law function.

The size is normalized with respect to the Fresnel radius. It turns out that the curve of scintillation level vs. size, peaks for a size about 1.05 (the Fresnel radius). That is, the maximum effect occurs for those irregularity sizes that are close to the Fresnel radius, as is to be expected. Since the curve drops off very sharply on both sides, the assumption of a gaussian distribution is a reasonable approximation for observations in any particular frequency providing that the gaussian scale size is taken as approximately the Fresnel radius. The difficulty, of course, is that the Fresnel radius is itself a function of frequency and of the distance between the receiver and the scattering irregularity. These results also explain the tendency of the earlier workers to find scale sizes close to what one would compute for the Fresnel radius for their particular observing conditions.

These results suggest a means of providing a simple modification to the existing model for frequency extrapolation. One could, for instance, compute the irregularity model for a particular set of circumstances using a convenient standard frequency near 100 MHz. These results would give the magnitude of the irregularity corresponding to the Fremouw radius for that frequency. This magnitude could then be inserted into the size distribution function to obtain the magnitude of the irregularity for the Fresnel radius at the desired frequency. The model could then be used as it stands to obtain the approximate scintillation index appropriate for that frequency. This approach was not pursued nor tested because the major interest is in extrapolating frequencies to the SHF band. The method proposed would not be appropriate if the recently reported Booker theory on SHF equatorial scintillations is determined to be correct. It could, however, be used to extrapolate scintillation effects to frequencies up to 1 GHz.

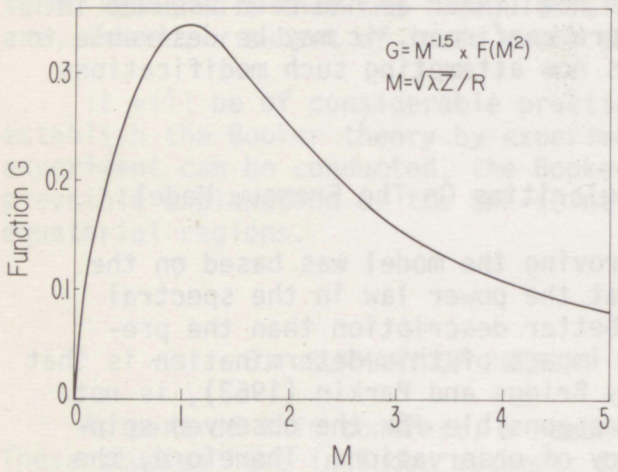

Figure 1. Frequency dependent portion of the Briggs and Parkin (1963) theory as modified to include a power law irregularity distribution.

5.3. Steep Front Electron Density Interference Patterns

One type of interference pattern that has similarities to scintillations is that produced by steep discontinuities in F region electron density. The pattern received is usually characterized by onset of a rapidly oscillating signal whose amplitude increases with time and as the period of oscillations decreases. This "ringing" effect is then often followed by a period of the order of 10 seconds of signal dropout which, in turn, is followed by a ringing phenonemon, inverse, but otherwise similar to the first ringing effect. This effect was discussed by Elkins & Slack (1969) who included a qualitative theory.

The effect was recently noted on charts obtained at the ERL Boulder ATS-6 radio beacon station. Figure 2 shows the event as recorded in the three radio beacon frequencies. Figure 3 is a tracing of a computer plot showing the signal at 360 MHz at high resolution. Because of its similarity to scintillation effects, and because it may have some practical importance, a detailed quantitative theory of the phenomenon was developed, to be tested against the observations. The theoretical development is contained in the Appendix. Unfortunately, the theory has not yet been quantitatively compared with the observational results although it appears capable of explaining the main details observed in the signal.

According to the theory, the phenomenon is produced by a discontinuity that moves across the ray path between the satellite and the surface station producing a two-ray interference pattern. Ultimately, the discontinuity is interposed between the satellite and the observer, in which case one of two things will happen: either a transmitted ray will be observed, or a complete

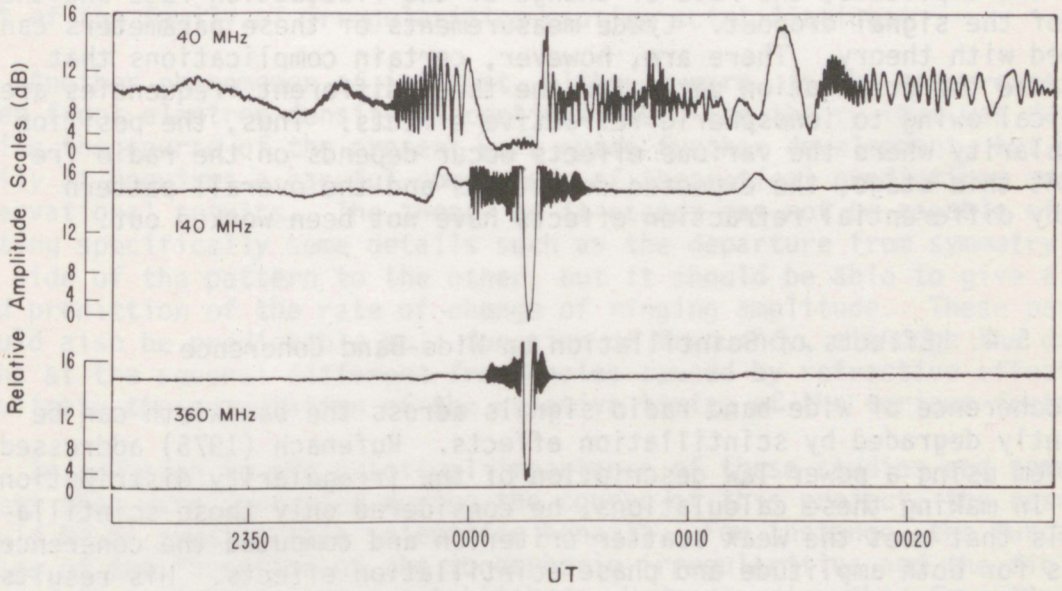

Figure 2. Example of the steep front "ringing" phenomenon observed at the Boulder ATS-6 radio beacon station on 40, 140, and 360 MHz.

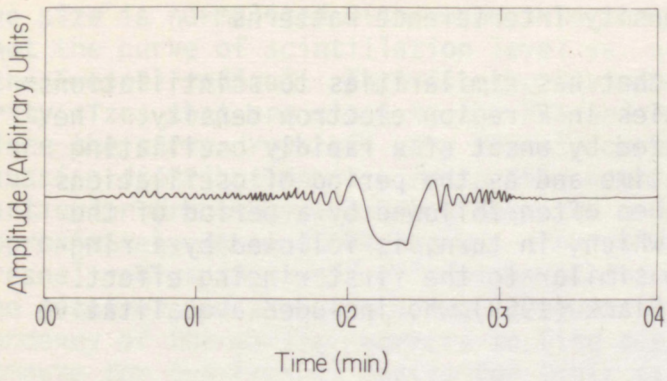

Figure 3. Tracing of a computer-produced plot showing time scale expansion of the 360 MHz record of figure 2.

signal dropout will occur. The occurence of the signal dropout depends on whether the ray to the plane of the discontinuity is greater than, or less than, the critical angle of reflection at the particular radio frequency and the particular electron density change. If the angle is less than the critical angle, the ray is totally reflected out of the range of the receiver and the discontinuity appears opaque to the station. As the discontinuity moves out of the direct ray path, a two-ray interference pattern again develops by means of reflection from the back interface of the discontinuity. The theory shows that a number of variations in the characteristics of the event may occur depending on certain geometrical configurations and on whether the ray to the discontinuity undergoes a critical reflection.

Fortunately, the observations on ATS-6 radio beacon are made at several radio frequencies. These include 40, 140, and 360 MHz. At the present stage in theoretical development, it is possible to predict certain frequency-dependent features of the ringing phenomenon. These include the rate of change of the amplitude, the rate of change of the fluctuation rate and the duration of the signal dropout. Crude measurements of these parameters can be compared with theory. There are, however, certain complications that arise because the propagation paths for the three different frequencies are not identical owing to ionospheric refractive effects. Thus, the position of the irregularity where the various effects occur depends on the radio frequency. At this stage, the expected deviations and the overall pattern produced by differential refraction effects have not been worked out.

5.4. Effects of Scintillation on Wide-Band Coherence

The coherence of wide-band radio signals across the bandwidth can be significantly degraded by scintillation effects. Rufenach (1975) addressed this problem using a power law description of the irregularity distribution in size. In making these calculations, he considered only those scintillation levels that meet the weak scatter criterion and computed the coherence properties for both amplitude and phase scintillation effects. His results show that the phase coherence is less dependent than the amplitude coherence on bandwidth and spectral size properties of the irregularities. This result suggests that wide-band phase-modulated systems would suffer less degradation due to scintillation effects than would amplitude modulated systems.

6. RECOMMENDATIONS FOR FURTHER STUDIES

The problem of primary practical importance in scintillations has to do with the equatorial GHz scintillation effects. From a theoretical point of view, the Booker hypothesis seems to be the most plausible explanation for the occurrence and magnitude of the equatorial GHz scintillation effects. The present observational evidence can neither definitively support nor rule out Booker's hypothesis. If his hypothesis is indeed valid, it would be fruitless to attempt frequency extrapolation of the present model of scintillation effects that are based on past observations primarily in the VHF range. Although, in principal, it would be possible to model the GHz scintillations empirically by further SHF observations, it would be better to devise models based on an understanding of the field-aligned irregularities themselves.

Experiments designed to test the Booker hypothesis crucially are therefore of utmost importance. Such experiments could, for instance, consist of specific simultaneous measurements of scintillations from geostationary sources and of scintillations observed during the passage of orbiting satellites using the same frequencies. The coincidence of scintillation activity with the passage of the orbiting satellite when it is in the vicinity of the ionospheric penetration point from the geostationary satellite is, of course, of low probability. It may, therefore, be necessary to apply a statistical treatment in which the average scintillation levels from low orbiting satellites are compared with those from geostationary satellites in a given frequency band.

Further studies of the HF duct type of field-aligned irregularities need to be conducted. Attempts should be made to determine if these ducts are part of the family of irregularities causing scintillations.

Another phenomenon of interest, although rare, is the occurrence of steep front electron density discontinuities. The theory that was developed during the course of the present work needs further development, but primarily it requires a careful comparison of theoretical predictions and the observational results. The theory as it stands may not be capable of predicting specifically some details such as the departure from symmetry from one side of the pattern to the other, but it should be able to give a fairly good prediction of the rate of change of ringing amplitude. These parameters should also be predictable as a function of frequency, although the different paths at the several different frequencies caused by refractive effects will complicate the computation of the relative timing of the various features.

In addition to the practical importance of these studies and some of the others that were conducted during the course of this project, the results should be of considerable scientific benefit. For instance, the fundamental causes of the formation of the ionospheric irregularities and the field aligned ducts have not been established. Understanding this formation is one of the more significant problems in ionospheric and magnetospheric physics, and it is expected that continuation of the studies may provide a basis for further theoretical developments of the generation mechanisms.

7. ACKNOWLEDGMENTS

The authors appreciate the efforts of several SEL staff in conducting this work; these include A. Paul, K. Davies, R. Fritz, and A. G. Jean. The support and technical discussions on the part of T. Golden and D. Levin, NASA, are also very much appreciated. Financial support for this joint NOAA/NASA program was supplied in part under NASA work statement 5-50871-AG.

8. PUBLICATIONS RESULTING FROM PRESENT STUDY

During the course of this joint NASA/NOAA funded study, a number of papers were published or presented at scientific meetings. These are listed below:

Pope, J. H. (1974): Global scintillation model, NOAA Technical Report ERL 308-SEL 30, U. S. Government Printing Office, Washington, D. C. 20402.

Pope, J. H. (1974): The use of global ionospheric irregularity models for satellite communications, NTC'74 Record (IEEE Publication 74CH0902-7 CSCB), 292-295.

Pope, J. H. (1974): Review of a global scintillation model and its modifications, URSI Comm 6, Special Session on Communication Channels with Emphasis on UHF Satellite Links, Boulder, Colorado, 11-17 October.

Rufenach, C. L. (1975): Ionospheric scintillation by a random phase screen: Spectral approach, *Radio Science* 10: 155-165.

Rufenach, C. L. (1975): Coherence properties of wideband satellite signals caused by ionospheric scintillation, *Radio Science* (to appear in Nov. 1975 issue)

Rufenach, C. L. (1975): On the variation of radio scintillation spectral shape with geometry, *J. Atmos. Terr. Phys.* (Submitted).

9. REFERENCES

Aarons, J. (1973): A descriptive model of F-layer high latitude irregularities as shown in scintillation observations, *J. Geophys. Res.* 78:7441-7450.

Aarons, J., and R. Allen (1971): Scintillation boundary during quiet and disturbed mangetic conditions, *J. Geophys. Res.* 76:170-177.

Booker, H. G. (1958): The use of radio stars to study irregular refraction of radio waves in the ionosphere, *Proc. IEEE* 46:298-314.

Booker, H. G. (1975): The Role of the Magnetosphere in Satellite and Radio-Star Scintillation, in *Proceedings*, 1975 Symposium on the Effect of the Ionosphere on Space Communications, January 20-22, 1975, Arlington, VA, Naval Research Laboratory.

Bowhill, S. A. (1961): Statistics of a radio wave diffracted by a random ionosphere, *J. Res. NBS* 65D:275-292.

Briggs, B. H., and I. A. Parkin (1963): On the variation of radio star and satellite scintillations with zenith angle, *J. Atmos. Terr. Phys.* 25:339-365.

Chivers, H. J. A., and R. D. Davies (1962): A comparison of radio star scintillations at 1390 and 79 Mc/s at low angles of elevation, *J. Atmos. Terr. Phys.* 24:573-584.

Christiansen, R. M. (1971): Preliminary report of S-band propagation disturbance during ALSEP mission support (November 19, 1969-June 30, 1970), NASA Report No. X-861-71-239.

Craft, H. D., Jr., and L. H. Westerlund (1972): Scintillations at 4 and 6 GHZ caused by the ionosphere, AIAA Paper No. 72-179, presented at AIAA 10th Aerospace Sciences Meeting, San Diego, Calif., January 17-19, 1972.

Dyson, P. L. (1969): Direct measurements of the size and amplitude of irregularities in the topside ionosphere, *J. Geophys. Res.* 74:6291-6303.

Dyson, P. L., J. P. McClure, and W. B. Hanson (1974): In situ measurements of amplitude and scale size characteristics of ionospheric irregularities, *J. Geophys. Res.* 79:1497-1502.

Elkins, T. J. and F. F. Slack (1969): Observations at travelling ionospheric disturbances using stationary satellites, *J. Atmos. Terr. Phys.* 31:421-439.

Fremouw, E. J., and C. L. Rino (1973): An empirical model for average F-layer scintillation at VHF/UHF, *Radio Sci.* 8:213-222.

Fremouw, E. J., and C. L. Rino (1974): Modeling of transionospheric radio propagation, Quarterly Technical Report 1, Stanford Research Institute Project 3416.

Helliwell, R. A., J. H. Crary, J. H. Pope, and R. L. Smith (1956): The 'nose' whistler - a new high latitude phenomenon, *J. Geophys. Res.* 61:139-142.

Joint Satellite Studies Group (1968): On the latitude variation of scintillations of ionosphere origin in satellite signals, *Planet. Space Sci.* 16:775-781.

Loftus, B. T., T. E. VanZandt, and W. Calvert (1966): Observations of conjugate ducting by the fixed-frequency topside-sounder satellite, *Ann. Geophys.* 22:530-537.

Lovelace, R. V. E., E. E. Salpeter, L. E. Sharp, and D. E. Harris (1970): Analysis of observations of interplanetary scintillations, *Astrophys. J.* 159:1047.

McClure, J. P., and W. B. Hanson (1973): A catalog of ionospheric F region irregularity behavior based on OGO 6 retarding potential analyzer data, *J. Geophys. Res.* 78:7431-7440.

Muldrew, D. B. (1967): Medium frequency conjugate echoes observed on topside-sounder data, *Can. J. Phys.* 45:3935-3944.

Muldrew, D. B. (1963): Radio propagation along magnetic field-aligned sheets of ionization observed by the Alouette topside sounder, *J. Geophys. Res.* 68:5355-5370.

Pope, J. H. (1974a): High latitude ionospheric irregularity model, *Radio Sci.* 9:675-682.

Pope, J. H. (1974b): Global scintillation model, NOAA Tech. Report ERL 308-SEL 30.

Pope, J. H. (1974c): The use of global ionospheric irregularity models for satellite communications, NTC '74 Record (IEEE Publication 74CH0902-7 CSCB), 292-295.

Pope, J. H., and R. B. Fritz (1970): Observations of simultaneous scintillation on VHF and S-band satellite transmissions at high latitudes, NOAA Tech Report ERL 207-OD 6.

Pope, J. H., and R. B. Fritz (1971): High latitude scintillation effects on very high frequency (vhf) and S-band satellite transmissions, *Indian J. Pure Appl. Phys.* 9:593-600.

Rufenach, C. L. (1971): A radio scintillation method of estimating the small-scale structure in the ionosphere, *J. Atmos. Terr. Phys.* 33:1941-1951.

Rufenach, C. L. (1972): Power-law wavenumber spectrum deduced from ionospheric scintillation observations, *J. Geophys. Res.* 77:4761-4772.

Rufenach, C. L. (1975): Coherence properties of wideband satellite signals caused by ionospheric scintillation, *Radio Science* (to appear in Nov. 1975 issue)

Sagalyn, R. C., M. Smiddy, and M. Ahmed (1974): High latitude irregularities in the topside ionosphere based on ISIS-1 thermal ion probe data, *J. Geophys. Res.* 79:4252-4261.

Singleton, D. G. (1974): Power spectra of ionospheric scintillations, *J. Atmos. Terr. Phys.* 36:113-133.

Skinner, R. F. Kelleher, J. B. Hacking, and C. W. Benson (1971): Scintillation fading of signals in the SHF band, *Nature, Phys. Sci.* 232:19-21.

Taur, R. R. (1973): Ionospheric scintillations at 4 and 6 GHz, *COMSAT Tech. Rev.* 3:145-163.

Taur, R. R. (1974): Ionospheric scintillation at frequencies above 1 GHz, *COMSAT Tech. Rev.* 4:461-476.

APPENDIX

RADIO INTERFERENCE PATTERNS CAUSED BY DISCONTINUITIES IN IONOSPHERIC ELECTRON DENSITIES

1. INTRODUCTION

On rare occasions a particular type of interference pattern is noted on signals originating from geostationary satellites, (Elkins and Slack, 1969). These interference patterns are characterized by a "ringing" effect with an increasing amplitude followed by a signal dropout and then by another ringing effect that is approximately symmetrical with the first but with a decreasing amplitude. The entire event lasts about 10 minutes. On a few occasions these events have been recorded in Boulder from the ATS-6 radio beacon. The surprising characteristic of these events is the nearly complete signal dropout that may last several minutes.

The effect has been explained qualitatively (Elkins and Slack, 1969), but no quantitative discussion of the effect has been reported. The suggestion is that the event is caused by a steep, nearly discontinuous, gradient in electron density moving across the satellite ray path to surface station. The ringing effect is produced essentially by the two-ray interference pattern between the reflected and direct rays from the surface of the discontinuity. The signal dropout is produced when the conditions are such that the transmitted ray is blocked when the angle of incidence to the surface is smaller than the critical angle of reflection.

2. THEORY

The amplitude coefficients of reflection of a radio wave incident on a discontinuous boundary in refractive index is given by (Budden, 1961)

$$R_{||} = \frac{n_2^2 \operatorname{Sin}\Theta - n_1 (n_2^2 - n_1^2 \operatorname{Cos}^2\Theta)^{\frac{1}{2}}}{n_2^2 \operatorname{Sin}\Theta + n_1 (n_2^2 - n_1^2 \operatorname{Cos}^2\Theta)^{\frac{1}{2}}} \qquad (1)$$

and

$$R_{\perp} = \frac{n_1 \text{ Sin } \theta - (n_2^2 - n_1^2 \text{ Cos } ^2\theta)^{\frac{1}{2}}}{n_1 \text{ Sin } \theta + (n_2^2 - n_1^2 \text{ Cos } ^2\theta)^{\frac{1}{2}}} \qquad (2)$$

where $R_{||}$ = reflection coefficient of the wave having electric vector parallel to the surface,

$R_{\perp}$ = reflection coefficient of the wave having electric vector perpendicular to the surface,

θ = angle of incidence measured from the surface

n_1 = refractive index of the medium in which the ray is propagating,

n_2 = refractive index of the medium upon which the ray is incident.

The geometrical relationships are shown in figure A.1. Note that the angles of incidence and reflection in this development are defined as the complementary angles as defined by Budden; hence, minor changes in the equations occur.

For the problem at hand several approximations are appropriate. One of these is possible because for the frequencies of interest (40, 140, and 360 MHz) the critical angle of reflection is small. Thus, the entire event can be considered as occurring when the angle of incidence is less than 1/10th radian so that the usual trigonometric small angle approximations can be made (i.e., Sin $\theta = \theta$). Also, the index of refraction is approximated as equal to 1 and the change in the index across the surface is approximated as very much less than 1. Under these approximations the reflection coefficients for the two polarizations are nearly equal and are given by

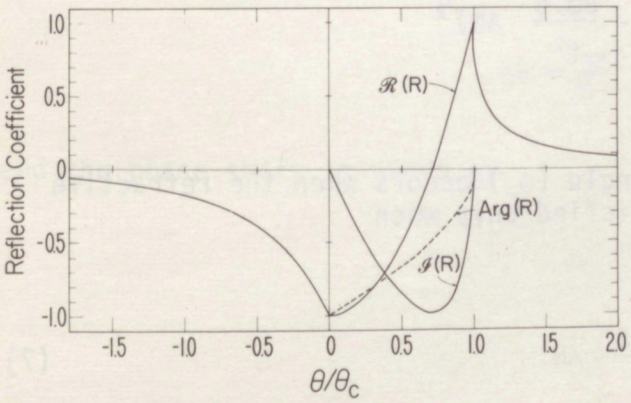

Figure A.1. Reflection coefficient of the two sides of a steep front discontinuity as a function of reflection angle θ normalized by the critical angle θ_c. The reflection coefficient is complex for $0 < \theta/\theta_c < 1$; the real and imaginary components and the argument of the reflection coefficient are plotted in that region.

$$R_{||,\perp} = \frac{\theta - (2\varepsilon + \theta^2)^{\frac{1}{2}}}{\theta + (2\varepsilon + \theta^2)^{\frac{1}{2}}} \tag{3}$$

where θ = angle of incidence and

ε = change in refractive index from one region to the next (i.e., $\varepsilon = n_2 - n_1$).

For refractive index nearly equal to unity we can write:

$$\eta \simeq 1 - \frac{40.25}{f^2} N \tag{4}$$

and

$$\varepsilon = \frac{40.25}{f^2} \Delta N \tag{5}$$

where N = electron density (electrons/m^3),

ΔN is change in electron density across the boundary, and

f = frequency (Hz).

Then (3) becomes

$$R = \frac{\theta - (\theta^2 - \frac{80.5}{f^2} \Delta N)^{\frac{1}{2}}}{\theta + (\theta^2 - \frac{80.5}{f^2} \Delta N)^{\frac{1}{2}}} \quad . \tag{6}$$

The angle known as the critical angle (θ_c) occurs when the refractive index is unity. This condition is satisfied only when

$$\theta_c = \frac{80.5}{f^2} \Delta N \tag{7}$$

and is non-imaginary only for positive ΔN, i.e., for an enhancement in electron density from the first to second regions, N_2 is less than N_1. It is convenient to rewrite (6) as:

$$R = \frac{\theta - (\theta^2 - \theta_c^2)^{\frac{1}{2}}}{\theta + (\theta^2 - \theta_c^2)^{\frac{1}{2}}} \tag{8}$$

Equation (8) shows that the reflection coefficient for $0 < \theta < \theta_c$ is complex and hence must be treated in a special manner in computing the interference effects from rays within this region. To the left of the boundary where the electron density is greater than in the first region, the reflection coefficient is real but negative. This fact implies that a phase change of π radians must be added to the phase derived from the geometrical relationships. The reflection coefficient in each of these three regions ($\theta > \theta_c$, $0 \leq \theta < \theta_c$, and $\theta < 0$) is shown in Figure A.2 as a function of the angle of incidence normalized by the critical angle. In the region $0 \leq \theta < \theta_c$, the real and imaginary components of the complex reflection coefficient are shown along with the argument of the reflection coefficient. The argument is given by the expression

$$\text{ARG}(R) = \tan^{-1}\left(\frac{\mathcal{I}}{\mathcal{R}}\right) \tag{9}$$

where $\mathcal{R}$ and $\mathcal{I}$ respectively are the real and imaginary components of the reflection coefficient.

From the geometric construction given in Figure A.1 we can derive the phase difference between the direct and reflected signal in terms of the range to the irregularity when it is directly in the ray path (h) and the perpendicular distance of irregularity from the direct ray path (x). Assuming that $x << h$ the binomial approximations hold and we find that the change in the range (Δh) is given by

$$\Delta h = \frac{\frac{1}{2}x^2}{h} , \tag{10}$$

and the phase shift is given by

$$\Phi = 2\pi\left(\frac{\Delta h}{\lambda}\right) . \tag{11}$$

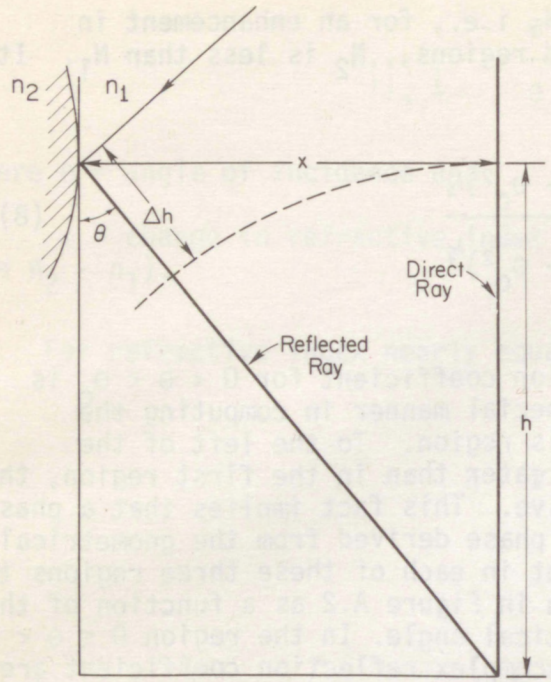

Figure A.2. The geometry and nomenclature relating to the two-ray interference pattern are shown where the reflected ray, propagating in a medium of electron density n_1, is reflected by a steep front having electron density n_2.

The angle subtended between the direct and the reflected rays as observed on the surface is Θ' and is given, in the small angle approximation, by

$$\Theta' = \frac{x}{h} \quad . \tag{12}$$

Taking the derivative of both sides gives the change in the phase with respect to x. Then

$$d\Phi = 2\pi \frac{x}{h} \frac{f}{c} dx. \tag{13}$$

The wavelength τ of the interference pattern on the chart occurs as an integer multiple of 2π . Thus the period can be written from

$$\Delta x = \frac{hc}{xf} \tag{14}$$

where Δx is the transverse distance moved by the structure to produce one cycle change in the pattern. The time interval as measured on the chart is, of course, directly proportional to Δx.

A special case of interest occurs when $\theta' = \theta_c$. Equation (13) becomes

$$\Delta x_c = \frac{c}{\sqrt{80.5\ \Delta N}} \quad . \tag{15}$$

Thus for this case the interference pattern period is independent of frequency or of the geometric relationships but is dependent on only the change in electron density. If we can identify this special case on the observed pattern, this fact may provide a measure of the effective electron density step. We can then use the value of ΔN so determined in the equations for reflection coefficient to check for consistency.

Depending on the circumstance, we can identify several different cases, each of which would have a specific characteristic signature in the overall pattern. The simplest case occurs when the plane of the discontinuity is parallel to the ray path in the line of sight to the satellite. Three regions of the pattern can be identified. The first of these (Region 1) occurs when $\theta \geq \theta_c$ and we get the usual increasing interference ringing effect. Region 2 occurs when $0 \leq \theta < \theta_c$. From this condition an interference pattern will be produced that is associated with the complex refractive index. Region 3 occurs when $\theta \leq 0$, producing a ringing pattern that is characteristic of the backside of the discontinuity with an increased electron density. In this particular case there will be no signal dropout associated with the event. In general, the ringing patterns to either side of the front are not strictly symmetrical.

Other cases occur when there is a tilt in the front of the discontinuity with respect to the ray path. In this event there are two possibilities. One is that the angle of the tilt is less than the critical angle and the other is that it is greater than the critical angle. The latter can be referred to as Case 3 and the former, Case 2. In general for Case 2, Region 1 will be the same as in Case 1. Region 2 will be confined to $\theta \leq \theta_c$ but greater than some angle that depends on the angle of the tilt. In this region, the wave form will correspond to the Region 2 above in Case 1. However, a fourth region (Region 4) will occur where the signal drops essentially to zero as the ray path is occluded by the ionospheric structure. Since the angle of incidence is within the critical angle, there is no transmitted wave and the occlusion prevents the direct ray from reaching the receiver. As the front passes to the other side of the ray path, the region will again be reached where $\theta < 0$, producing the fourth region corresponding to Region 3 of Case 1.

Case 3 is such that the angle of the wave front, when it is in the discontinuity front, is greater than the critical angle. Thus, Case 3 will differ from Case 2 in Region 3. In Case 3, as the structure occludes the ray, a transmitted wave is allowed, the magnitude of which depends on the transmission coefficient which is a function of incidence angle. However, as the

event progresses, a position is reached such that the angle of incidence becomes equal to or less than Θ_c. The transmitted wave then becomes occulted as in Case 2 and the event becomes identical to Region 4 of Case 2. Other variations may occur. For instance, only one side or the other of the ringing pattern might be observed.

As mentioned before, the ringing pattern from one side to the other of the irregularity will in general be non-symmetrical. A further cause for failure of the pattern to be symmetrical can be produced by the pattern having a considerable motion in the direction of the ray path. This component could produce geometrical relationships sufficiently different for the duration of the event that the pattern would appear non-symmetrical.

In this analysis the usual approximation pertaining to geostationary satellites, that the satellite can be considered at an infinite distance from the observer, is not valid. Owing to the small critical angles associated with this phenomenon, a slight change in the angle to the satellite, as the front moves in respect to the ground station, becomes significant. Indeed, observation of the ringing phenomenon on both sides of the event is possible only if the approximation does not hold. In addition, a slight curvature of the front must be postulated in order that some point can always be found such that the angle of reflection is equal to the angle of incidence. If the front were strictly plain there would be only one point on each side of the ray path where it would be possible to observe the ringing phenomenon. A real event would be more likely to have a finite radius of the curvature than to be strictly flat. This radius of curvature can be large enough that effects of ray convergence and divergence can be ignored and still satisfy the conditions of this problem.

For Case 3, we can obtain the relationship between the duration of the signal dropout and observing frequency. Multiple frequency observation can then provide a check on the hypothesis. The dropout occurs during the interval that $0 \leq \Theta \leq \Theta_c$. The time of dropout then is linearly related to the time required for Θ to change from Θ_c to 0. In the small angle approximation the length of that time interval is proportional to Θ_c. From (7) we obtain

$$\Theta_c = \sqrt{80.5\ \Delta N}\ \frac{1}{f} \quad . \tag{16}$$

Thus if the pattern signature is sufficiently clear that we can recognize an event of Case 3, we should find an inverse relationship of the dropout duration and frequency.

☆U.S. GOVERNMENT PRINTING OFFICE: 1975—677-347/1221 REGION NO. 8

ENVIRONMENTAL RESEARCH LABORATORIES

The mission of the Environmental Reasearch Laboratories is to study the oceans, inland waters, the lower and upper atmosphere, the space environment, and the earth, in search of the understanding needed to provide more useful services in improving man's prospects for survival as influenced by the physical environment. Laboratories contributing to these studies are:

Atlantic Oceanographic and Meteorological Laboratories (AOML): Geology and geophysics of ocean basins and borders, oceanic processes, sea-air interactions and remote sensing of ocean processes and characteristics (Miami, Florida).

Pacific Marine Environmental Laboratory (PMEL): Environmental processes with emphasis on monitoring and predicting the effects of man's activities on estuarine, coastal, and near-shore marine processes (Seattle, Washington).

Great Lakes Environmental Research Laboratory (GLERL): Physical, chemical, and biological, limnology, lake-air interactions, lake hydrology, lake level forecasting, and lake ice studies (Ann Arbor, Michigan).

Atmospheric Physics and Chemistry Laboratory (APCL): Processes of cloud and preciptation physics; chemical composition and nucleating substances in the lower atmosphere; and laboratory and field experiments toward developing feasible methods of weather modification.

Air Resources Laboratories (ARL): Diffusion, transport, and dissipation of atmospheric contaminants; development of methods for prediction and control of atmospheric pollution; geophysical monitoring for climatic change (Silver Spring, Maryland).

Geophysical Fluid Dynamics Laboratory (GFDL): Dynamics and physics of geophysical fluid systems; development of a theoretical basis, through mathematical modeling and computer simulation, for the behavior and properties of the atmosphere and the oceans (Princeton, New Jersey).

National Severe Storms Laboratory (NSSL): Tornadoes, squall lines, thunderstorms, and other severe local convective phenomena directed toward improved methods of prediction and detection (Norman, Oklahoma).

Space Environment Laboratory (SEL): Solar-terrestrial physics, service and technique development in the areas of environmental monitoring and forecasting.

Aeronomy Laboratory (AL): Theoretical, laboratory, rocket, and satellite studies of the physical and chemical processes controlling the ionosphere and exosphere of the earth and other planets, and of the dynamics of their interactions with high-altitude meteorology.

Wave Propagation Laboratory (WPL): Development of new methods for remote sensing of the geophysical environment with special emphasis on optical, microwave and acoustic sensing systems.

Marine EcoSystem Analysis Program Office (MESA): Plans and directs interdisciplinary analyses of the physical, chemical, geological, and biological characteristics of selected coastal regions to assess the potential effects of ocean dumping, municipal and industrial waste discharges, oil pollution, or other activity which may have environmental impact.

Weather Modification Program Office (WMPO): Plans and directs ERL weather modification research activities in precipitation enhancement and severe storms mitigation and operates ERL's research aircraft.

NATIONAL OCEANIC AND ATMOSPHERIC ADMINISTRATION
BOULDER, COLORADO 80302